Environmental Science and Pollution Research (2021) 28:16895–16912
https://doi.org/10.1007/s11356-020-11995-3

RESEARCH ARTICLE

Anthropogenic and climate induced trace element contamination in a water reservoir in northwestern Mexico

Roberto Ochoa-Contreras[1] · Martín Enrique Jara-Marini[2] · Joan-Albert Sanchez-Cabeza[3] · Diana María Meza-Figueroa[4] · Libia Hascibe Pérez-Bernal[3] · Ana Carolina Ruiz-Fernández[3]

Received: 24 July 2020 / Accepted: 7 December 2020 / Published online: 4 January 2021
© The Author(s), under exclusive licence to Springer-Verlag GmbH, DE part of Springer Nature 2021

Abstract

Water reservoirs are essential for regional economic development, as populations depend on them for agriculture irrigation, flood control, hydroelectric power generation, water supply for human consumption, and subsistence fishing activities. However, the reservoir environmental quality can be disturbed by enhanced sediment input and trace metal contamination, affecting human health as a consequence of contaminated water and fish consumption. With the purpose to understand the trends and extent of sediment accumulation and trace element contamination in the Oviachic reservoir (OV, northwestern Mexico) since its construction, the temporal variations of sediment accumulation, and As, Cr, Cu, Hg, Ni, Pb, and Zn concentrations, enrichment, and fluxes, were evaluated through the study of two ^{210}Pb-dated sediment cores. We assumed that siltation and trace element contamination were driven by the development of anthropogenic activities in the region within the past ~ 70 years. Elemental concentrations accounted from null to minor enrichment for most elements, but moderate to significant enrichment by Hg. Mercury, As, and Cu fluxes have notably increased since the past decade, most likely because of a combination of anthropogenic and natural processes, including catchment erosion, artisanal gold mining, and recent drought conditions in the region. Arsenic and Hg concentrations may pose deleterious risks to biota in the reservoir, and consequently to humans through fish consumption, for which further biological and toxicological tests are advisable. This study highlights the importance of using sediment dating to assess historical trends of metal contamination and identify possible sources, to support decision-making in programs addressed to reduce environmental and health risks in aquatic ecosystems.

Keywords ^{210}Pb dating · Sediment accumulation rates · Trace element contamination · Water reservoirs · Climate variability

Introduction

Population growth and anthropogenic activities are associated with environmental degradation owing to the exponential increase of land use change and contaminant inputs to aquatic ecosystems (Ciszewski and Grygar 2016; Reza and Singh 2010). Contamination by metals and metalloids is one of the major quality issues in aquatic reservoirs due to their persistence and potential for bioaccumulation and biomagnification (Peters et al. 2013; Mishra et al. 2019). These elements have both natural and anthropogenic sources. Although some of them are essential for metabolic functions in organisms (e.g., Cu, Fe, Mn, Ni, and Zn; Appenroth 2010), frequently, there is a small difference between biological benefits and toxicity, depending on biotic and non-biotic parameters (Qi et al. 2010; Mishra et al. 2019).

Discharges of improperly treated effluents from urban, industrial, agriculture, and mining activities deliver high loads of

Responsible Editor: Philippe Garrigues

✉ Ana Carolina Ruiz-Fernández
caro@ola.icmyl.unam.mx

[1] Posgrado en Ciencias, Centro de Investigación en Alimentación y Desarrollo, Unidad Hermosillo, Carretera Gustavo Astiazarán Rosas 46, Col. La Victoria, 83304 Hermosillo, Sonora, Mexico

[2] Centro de Investigación en Alimentación y Desarrollo, Unidad Hermosillo, Carretera Gustavo Astiazarán Rosas 46, Col. La Victoria, 83304 Hermosillo, Sonora, Mexico

[3] Instituto de Ciencias del Mar y Limnología, Unidad Académica Mazatlán, Universidad Nacional Autónoma de México, Calzada Montes Camarena s/n, Col. Playa Sur, 82040 Mazatlán, Mexico

[4] Departamento de Geología, División de Ciencias Exactas y Naturales, Universidad de Sonora, Rosales y Encinas, 83000 Hermosillo, Sonora, México

suspended solids and trace elements to continental aquatic ecosystems (Ruiz-Fernández et al. 2005). Surface runoff plays an important role in the transfer of contaminants through catchments to lakes and reservoirs. These contaminants eventually accumulate in sediments (Reza and Singh 2010) which conform to an archive of the historical contaminant deposition. ^{210}Pb dating has been used extensively to reconstruct the variation in contaminant inputs to aquatic reservoir sediments over the past 100–150 years (e.g., Ruiz-Fernández et al. 2004; Ontiveros-Cuadras et al. 2014; Méndez-García et al. 2016).

The Oviachic reservoir (OV, NW Mexico; Fig. 1) is one of the largest (~ 20,700 ha) in the region. It is at the lower reach

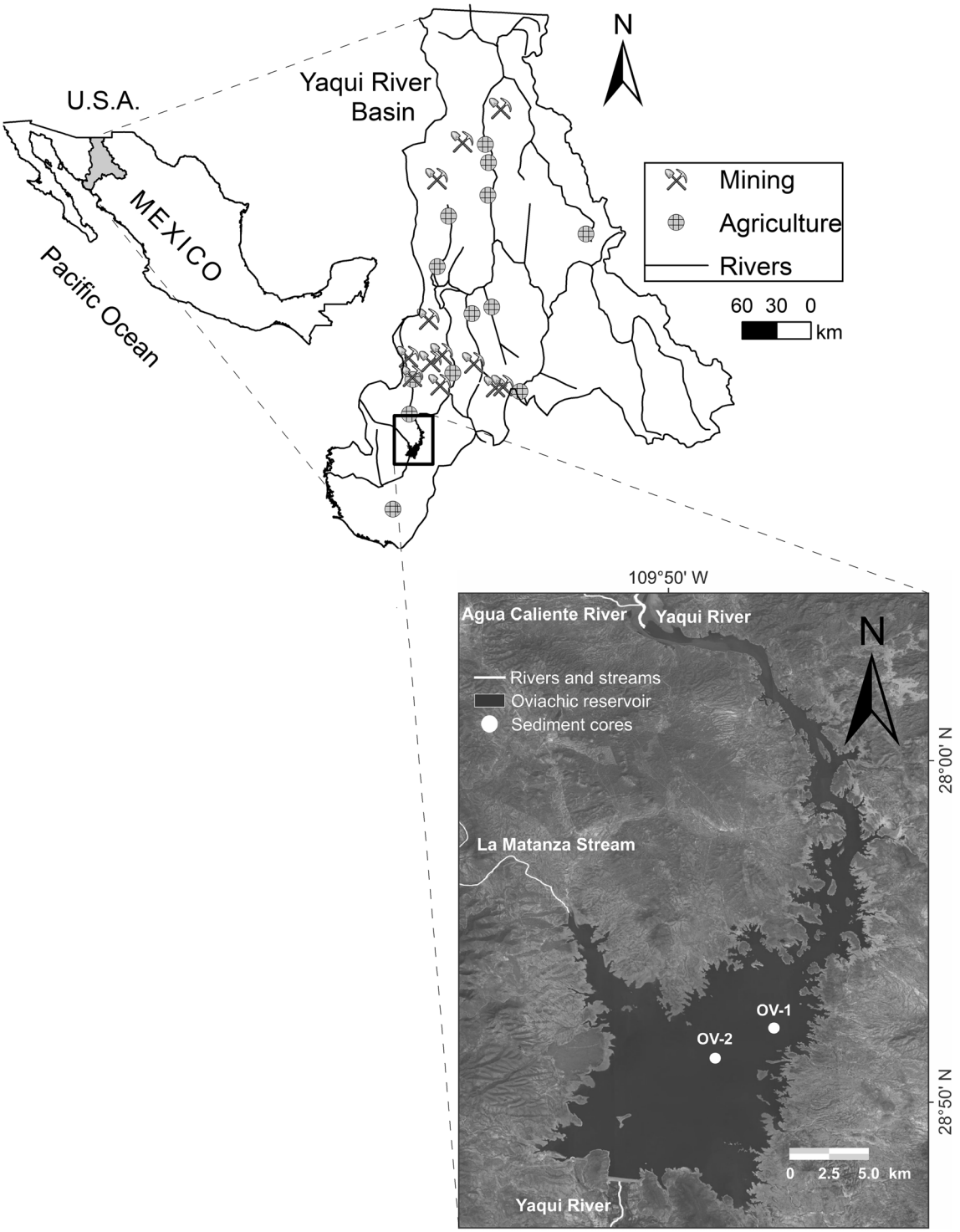

Fig. 1 Sampling sites at the Oviachic reservoir, Yaqui River Basin, Northwest Mexico

of the Yaqui River Basin receiving discharges from the entire watershed, in which three large reservoirs (including OV) and approximately 20 smaller reservoirs are established (Muñoz-Arriola et al. 2009). The OV is of high social and economic relevance, since it secures irrigation to the Yaqui Valley, which is the second most extensive agricultural area in Mexico (232,944 ha of irrigated surface, Enríquez and Durán 2017; CONAGUA 2020a). Metal and metalloid contamination and human health issues in the Yaqui River area have been related to large-scale application of agrochemicals (Guillette et al. 1998; Adler 2005; Cantú-Soto et al. 2009; Meza-Montenegro et al. 2012).

Mining is an ancestral activity in NW Mexico. Sonora State is currently the main producer of Cu and Mo in Mexico, contributing to a relevant proportion of Ag, Au, and Fe (SGM 2018). The Yaqui River region has consolidated over the last 20 years as the largest producer of Au and Cu in Mexico, increasing Cu production from 301,212 ton year^{-1} in 2000 to 655,807 ton year^{-1} in 2018 (INEGI 2018). Inadequately confined mine tailings are significant sources of trace element contamination in mining zones (USEPA 1997; Reza and Singh 2010). Ore deposits in the catchment include La Caridad mine, one of the largest open-pit Cu mines in the world. Some studies reported metal and metalloid dispersion to adjacent areas derived from water and wind erosion (Meza-Figueroa et al. 2009; De la O-Villanueva et al. 2013). Moreover, much large-scale and artisanal gold mining occurs in the mid-Yaqui River Basin (SGM 2018). Miners concentrate gold using Hg as a gold amalgamator, and this activity has recently increased (SEMARNAT-INECC 2017).

The main purpose of this study was to evaluate temporal changes of sedimentation rates and trace element (As, Cr, Cu, Hg, Ni, Pb, and Zn) concentrations and fluxes, as recorded in two ^{210}Pb-dated sediment cores from OV, under the hypothesis that changes in sedimentation and contamination are mostly driven by the recent development of major economic activities and population growth in the region.

Methods

Study area

The OV reservoir (also named Álvaro Obregón) is in Cajeme, southern Sonora State, ~ 37 km north of Obregón City (Fig. 1). The dam was built between 1947 and 1952 for flood control, irrigation of Yaqui Valley agriculture areas, power generation, and public water supply (CONAGUA 2018). It has an extension of 205 km^2, 57 m mean depth (CONAGUA 2008), and a maximum ordinary water level (MOWL) of 3023 hm^3, and it is located 105.5 m above sea level (SINA 2020). It is mainly fed by the Yaqui River, although it also receives the contributions of Agua Caliente River (through the Matanza stream; Fig. 1) and three aquifers (Cumuripa, Tecoripa, and Aguacaliente; CONAGUA 2015). OV is surrounded by rural areas; it supports recreational and subsistence fishing activities (carp, catfish, tilapia, and largemouth bass characterized mostly by benthic feeding habits). The Yaqui River has a natural surface runoff of 3148.2 hm^3 year^{-1} and a basin area of 74,640 km^2 (CONAGUA 2018), in which the mean precipitation is 527 mm year^{-1} (INEGI 2000).

North-south-oriented, low mountain ranges, separated by plains, characterize the area. The slopes are quite steep, especially in intrusive and metamorphic rocks, and the streams that drain this region promote intense erosion, producing lateral spurs that project into the plains (INEGI 2000). The Yaqui River Basin is mainly composed of rhyolite-acidic tuff (61% of the basin surface), alluvial soil (19%), and conglomerates (6%; Garrido-Hoyos 2019). The OV flood plain consists of conglomerates and agglomerates covered by alluvial terraces, outcropping basalts, and rhyolitic tuffs (SGM 2002). The main soil types in the area are cambisol, fluvisol, lithosol, regosol, vertisol, and xerosol (INAFED 2019). The climate in Cajeme is hot arid, predominantly desert (BW(h')w in 53.8% of the area) and steppe (BSo(h')w, in 34.5%), with a mean annual temperature above 18 °C and a dry winter (SEDESOL 2013). The precipitation occurs mainly from July to early September (Mexican monsoon season), and the average annual precipitation is 366.1 mm (INEGI 2017).

Sampling and analysis

Two sediment cores were collected in November 2018 (Fig. 1, Table 1) with a gravity corer (UWITEC™) using Plexiglas tubes (8.6 cm internal diameter and 1.5 m long). The sediment cores were extruded and sectioned into 1cm intervals. The core sections were freeze-dried at − 50 °C under vacuum (~ 0.1 mBar). Mass weight was recorded before and after drying. Samples were ground with a porcelain mortar and pestle (except aliquots for grain-size analysis).

Radiometric analyses were carried out every 4 cm depth along the cores, except for the bottom segments (below 57 cm depth in OV-1 and 45 cm depth in OV-2) where measurement resolution was every 2 cm. ^{210}Pb total (^{210}Pb$_{tot}$) activities were determined by alpha-particle spectrometry (Ortec Ametek Model 576A) through its descendant isotope ^{210}Po, assuming secular equilibrium between both radionuclides (Ruiz-Fernández and Hillaire-Marcel 2009). ^{226}Ra and ^{137}Cs activities were determined by gamma-ray spectrometry (Ortec Ametek High Purity Germanium well-detector; Ruiz-Fernández et al. 2014, Díaz-Asencio et al. 2020). Counting uncertainties ranged as follows: 5–6% for ^{210}Pb, 4–7% for ^{226}Ra, and 6–17% for ^{137}Cs. We assumed that supported ^{210}Pb (^{210}Pb$_{sup}$) was in equilibrium with its parent radionuclide ^{226}Ra. Excess ^{210}Pb (^{210}Pb$_{ex}$) corresponds to the difference between ^{210}Pb$_{tot}$ and ^{210}Pb$_{sup}$ (^{226}Ra).

Table 1 Sampling locations and dating information for sediment cores from the Oviachic reservoir, Yaqui River Basin, northwestern Mexico

Core	Location	Depth (m)	Core length (cm)	Maximum ^{210}Pb age (year)	SAR (cm year^{-1})	MAR (g cm^{-2} year^{-1})
OV-1	27° 53′ 09.6″ N 109° 49′ 35.1″ W	28	64.5	62.7 ± 0.8	0.39–2.67	0.13–0.47
OV-2	27° 52′ 54.0″ N 109° 49′ 47.0″ W	27	50	69.6 ± 0.7	0.34–2.48	0.13–0.38

Bulk geochemistry of sediments was determined at each core section in order to obtain a detailed record of the composition changes. Major and trace element sediment composition was determined by X-ray fluorescence spectrometry (XRF, Spectrolab Xepos-3) under helium atmosphere, using ~ 2 g of ground sediment placed into low-density polyethylene cells (bottom covered with Prolene film) and manually compressed with a Teflon rod. Hg concentrations were quantified by atomic absorption spectrophotometry (AAS; Varian SpectrAA-240FS) coupled to a cold vapor generator (Varian VGA-110), by using ~ 0.3 g of dry and ground sediments, which were acid digested (3:1 HCl and HNO_3) on a hotplate (80–100 °C, 5 h). The digestate was diluted with HPLC-grade water (Krishnamurty et al. 1976).

The sediments were also analyzed for grain-size distribution (sand, silt, and clay) by laser diffraction (Malvern Mastersizer 2000) on aliquots previously digested with 30% H_2O_2 to remove organic matter. For magnetic susceptibility (MS) measurements, we used a Bartington-MS2 equipment coupled to a MSG2 frequency sensor. Total carbon (C_{tot}) and nitrogen (N_{tot}), and the organic fraction of carbon (C_{org}) and nitrogen (N_{org}) concentrations, were analyzed with an Elementar Vario Micro Cube elemental analyzer. For the determination of the organic fraction, we used decalcified sediment aliquots, for which sediments were treated with 1 M HCl (drop by drop until no further effervescence was observed) and freeze-dried before analysis. The combustion temperature was 550 °C. The instrument was calibrated with the Soil Standard Silty B2182 and the High Organic Sediment Standard B2151 (Elemental Microanalysis Ltd.). Accuracy was assessed with the soil reference material Leco 502 697. The inorganic carbon fraction (C_{inorg}) was estimated from the difference between C_{tot} and C_{org}.

The accuracy assessment of methods included analysis of certified reference materials and control charts, in which the central value corresponds to the certified value for the analyte, and the upper and lower limits are the 95% confidence interval of the certified reference materials (CRM): IAEA-300 for ^{210}Pb and ^{137}Cs; IAEA-158, IAEA-405, and IAEA-433 for XRF; MESS-3 for AAS; LECO 502-309 for carbon and nitrogen concentrations; QAS3002 for grain-size distribution, and Bartington-G039 for MS. Moreover, all CRM analysis results are routinely checked through the Zeta-score approach (to compare measurements and CRM certified values; Kuselman and Fajgelj 2010). Results fell within the certified range values in the control charts, and the Zeta-score values were within the acceptable range of ± 2. Replicate analysis (n = 6) of a single sample showed that the variation coefficients were 5.8% for ^{210}Pb and 2.5% for ^{226}Ra and ^{137}Cs activities; 1.7% for Al, 2.6% for Ti, 2.8% for As, 5.4% for Cr, 5.7% for Cu, 4.5% for Ni, 2.9% for Pb, and 2.7% for Zn; 5.9% for C_{org}, C_{inorg}, and N concentrations; 6% for sand and clay, and 3% for silt percentages; and 3% for MS values.

Data treatment

^{210}Pb chronology

^{210}Pb chronologies, mass accumulation rates (MAR, g cm^{-2} year^{-1}), and sediment accumulation rates (SAR, cm year^{-1}) were calculated by using the constant flux (CF) model (Robbins 1978; Sánchez-Cabeza and Ruiz-Fernández 2012), and dating uncertainties were estimated by Monte Carlo simulation (Sanchez-Cabeza et al. 2014). ^{137}Cs activity profiles were used as stratigraphic markers to attempt the corroboration of the ^{210}Pb age models, assuming that the highest values correspond to the period of maximum ^{137}Cs fallout, caused by atmospheric thermonuclear weapon tests, during 1962–1964 (Robbins 1978).

Metal fluxes and flux ratio

Metal fluxes (μg cm^{-2} year^{-1}) derive from the product of the element concentration (μg g^{-1}) and MAR (g cm^{-2} year^{-1}) at each core section (Sanchez-Cabeza et al. (2014). The flux ratio, a concise representation of historical element inputs to an ecosystem (Heyvaert et al. 2000), was calculated as the quotient of modern to pre-dam construction fluxes for each sediment core.

Enrichment factor

We evaluated the degree of trace element contamination through the enrichment factor (EF) approach (Buat-Menard and Chesselet 1979). Probably, it is the most widely used and most successful enrichment indicator presently in use (Birch 2017). For each core section,

Table 2 Trace element concentration (μg g^{-1}), enrichment factor (EF), flux (μg cm^{-2} $year^{-1}$), and flux ratios in cores from Oviachic (OV) reservoir, Yaqui River Basin, northwestern Mexico

Core	Variable	As	Hg	Cr	Cu	Ni	Pb	Zn
OV-1	Concentration	25.9–42.2	0.16–0.97	24.8–45.9	60.6–77.0	24.9–31.7	45.3–83.8	108.3–154.4
	EF	0.95–1.7	0.83–5.8	0.83–1.4	0.83–1.2	0.84–1.1	0.83–1.6	0.85–1.1
	EF_{UCC}	5.3–9.5	2.8–19	0.28–0.45	2.0–2.9	0.50–0.65	2.5–4.9	1.6–2.1
	Flux	3.3–14.8	0.02–0.3	3.8–21.2	8.6–31.5	3.5–13.4	6.8–33.9	16.0–69.4
	Flux ratio	1.0–4.5	1.0–15.0	1.0–5.6	1.0–3.7	1.0–3.9	1.0–5.0	1.0–4.3
	Pre-dam*	26.8	0.17	30.6	68.6	27.9	52.3	129.2
OV-2	Concentration	24.7–41.7	0.13–0.70	23.7–48.3	58.8–77.1	24.6–30.7	37.7–83.1	98.6–157.8
	EF	0.80–1.6	0.46–3.0	0.62–1.0	0.81–1.2	0.88–1.1	0.64–1.6	0.87–1.1
	EF_{UCC}	4.7–9.1	2.3–15	0.27–0.45	1.9–2.9	0.50–0.66	2.0–5.1	1.7–2.1
	Flux	3.7–14.4	0.0–0.2	3.8–15.0	8.7–26.8	3.6–11.3	6.4–24.7	16.9–48.7
	Flux ratio	1.0–3.9	1.0–8.2	1.0–3.9	1.0–3.1	1.0–3.1	1.0–3.9	1.0–2.9
	Pre-dam*	28.1	0.25	32.0	67.7	27.1	53.7	127.8
UCC		4.8	0.05	92	28	47	17	67
TEL		5.9	0.174	37.3	35.7	18.0	35.0	123.0
PEL		17.0	0.486	90.0	197.0	36.0	91.3	315.0

UCC recommended upper continental crust concentrations (Rudnick and Gao 2004), *TEL* threshold effect level (Buchman 2008), *PEL* probable effect level (Buchman 2008)

*Pre-dam values are indicative of concentrations before dam construction

concentrations were normalized by Al, used as a reference element to compensate for variations of sediment grain size (Loring and Rantala 1992). Then, EF was calculated as the ratio of normalized element concentrations to pre-dam construction values (Table 2). Element pre-dam concentrations were estimated from the mean values in the three bottom sections of each core, nearly corresponding to the completion of the Oviachic reservoir. The EF was graded according to Essien et al. (2009): minor enrichment ($1.5 < EF < 3$), moderate enrichment ($3 < EF < 5$), and strong enrichment ($EF > 5$).

A second approach was also used to estimate the enrichment factor (EF_{UCC}) by considering the recommended upper continental crust values (Rudnick and Gao 2004) as background concentrations.

Sediment quality assessment

In order to assess the ecological significance of the trace element concentrations in OV, these were compared with the benchmarks threshold effect level (TEL; concentration at which adverse effects rarely occur) and probable effect level (PEL; concentration at which adverse effects occasionally occur) (Table 2; MacDonald et al. 2000).

Statistical analysis

Descriptive statistics (sample size, maximum, minimum, mean, and standard deviation) were calculated for geochemical characteristics and metal concentrations. Differences between mean values of the variables at each core were assessed through analysis of variance (ANOVA) with Tukey test at 95% of confidence ($p < 0.05$). Pearson's correlation analysis was performed to identify the association among variables analyzed, and significant correlation coefficients were identified through the Student's t test ($p < 0.05$).

Factor analysis (FA) was used to identify the primary sources of trace element variability in the dataset. The variables included the trace element concentrations (Al, As, Ca, Cr, Cu, Fe, Hg, Mn, Ni, Pb, Rb, Ti, Zn, and Zr) and the geochemical variables (MS, C_{org}, C_{inorg}, and grain-size fractions), for 115 observations (OV-1 and OV-2 sections). Significant variables within a factor should have at least a factor loading > |0.3| and a communality > 0.20 (Child 2006). In this study, the significant variables were those with loadings > |0.65| and communalities > 0.5.

Results

^{210}Pb chronology

$^{210}Pb_{tot}$ activities were similar between cores OV-1 and OV-2 ($p > 0.05$), ranging from 81.0 ± 5.2 to 183 ± 11 Bq kg^{-1}, and $^{210}Pb_{ex}$ activities from 30.4 ± 2.2 to 49.2 ± 2.6 Bq kg^{-1}. $^{210}Pb_{ex}$ activities in both cores decreased with depth, approximating exponential decay curves, with significant correlation

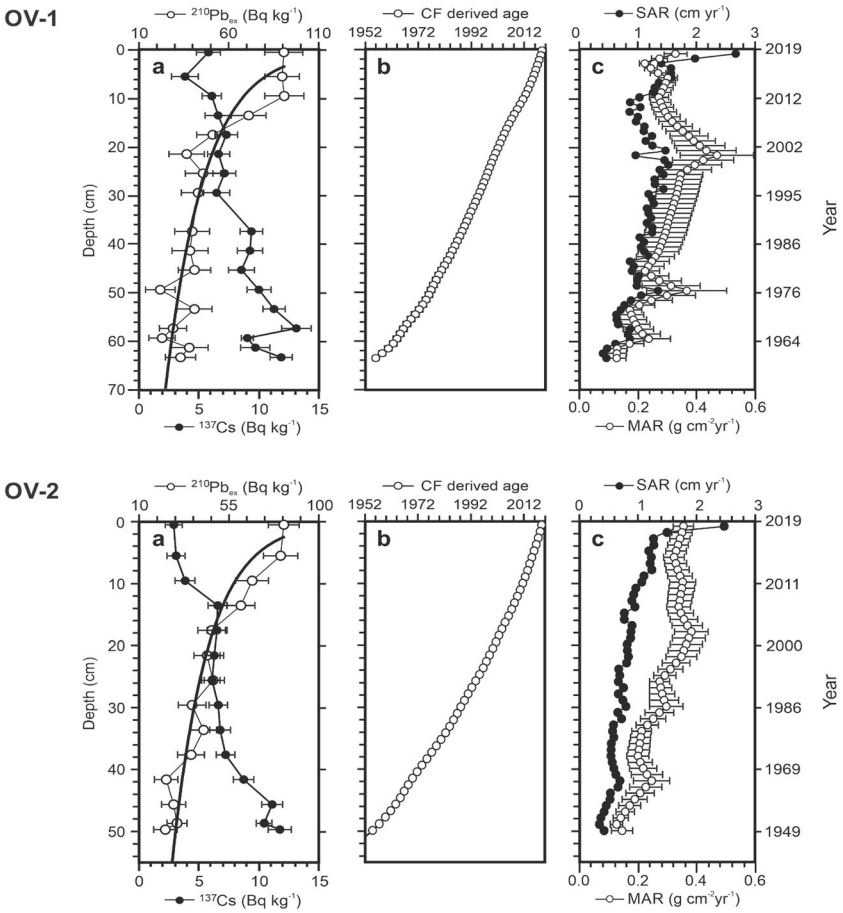

Fig. 2 Profiles of total ^{210}Pb and ^{137}Cs activities and accumulation rates of sediment cores from the Oviachic reservoir, Yaqui River Basin, Northwest Mexico

coefficients ($p < 0.05$): $r = 0.85$ in OV-1 and $r = 0.96$ in OV-2. However, in some core sections, $^{210}Pb_{ex}$ activities deviated from an exponential declining trend. As $^{210}Pb_{ex}$ did not reach equilibrium (where $^{210}Pb_{ex}$ activities approach zero), we estimated the missing $^{210}Pb_{ex}$ inventories at each core (14% for OV1 and 11% for OV2) (Appleby 1998; Sánchez-Cabeza and Ruiz-Fernández 2012). The bottom section ages were 62.7 ± 0.8 years (section 63–64 cm, dated 1956) for OV-1 and 69.6 ± 0.7 years (49–50 cm, 1949) for OV-2.

^{137}Cs activities were similar in both cores ($p > 0.05$), ranging from 3.9 ± 1.1 to 13.1 ± 1.2 Bq kg^{-1} for OV-1 and 2.9 ± 0.7 to 11.8 ± 1.0 for OV-2. ^{137}Cs activity profiles were also similar, with values decreasing upwards and a region with the highest but fluctuating values towards the core bottoms, below the section 57–58 cm (dated 1966 ± 1 year) in OV-1 and 45–46 cm (1960 ± 1 year) in OV-2 (Fig. 2).

MAR values were comparable between cores ($p > 0.05$), ranging from 0.13 ± 0.03 to 0.47 ± 0.13 g cm^{-2} year^{-1} for OV-1 and 0.13 ± 0.03 to 0.38 ± 0.06 g cm^{-2} year^{-1} for OV-2. SAR ranged from 0.39 ± 0.10 to 2.67 ± 0.32 cm year^{-1} for OV-1 and 0.34 ± 0.06 to 2.48 ± 0.24 cm year^{-1} for OV-2 (Table 1). Both SAR profiles (Fig. 2) showed increasing values from the past to reach maxima by the sampling year (2018), whereas MAR values showed subsurface maxima, with the highest value in between 2001 and 2002 (Fig. 2), more clearly observed in OV-1.

Sediment characterization

Both core sediments were predominantly clayey-silty (silt 43–67%, clay 33–56%) with very low (nil to 4%) and almost constant sand content. We observed transitions of clay and silt fractions (Fig. 3) at the upper sections (2002 to 2015 for OV-1 and 1985 to 2016 for OV-2).

C_{org} percentages were higher ($p < 0.05$) in OV-2 than OV-1, and values decreased with depth, approaching the typical exponential decay ($r = 0.69$ in OV-1 and $r = 0.85$ in OV-2) characteristic of C_{org} mineralization (Berner 1964). C_{inorg} percentages were low and also showed higher values up core. The molar ratios C_{org} to N_{org} (C:N) were highly variable (9.75–14.06 for OV-1 and 8.56–11.17 for OV-2) with comparable values between cores ($p > 0.05$). MS values were similar between cores ($p > 0.05$), with the lowest values at the core tops and the highest values in subsurface sections (10 to 25 cm, 1998–2011, in OV-1, and 10 to 32 cm, 1982–2011, in OV-2; Fig. 3). The concentration ranges of Al, Ca, Fe, Mn, Rb, Ti,

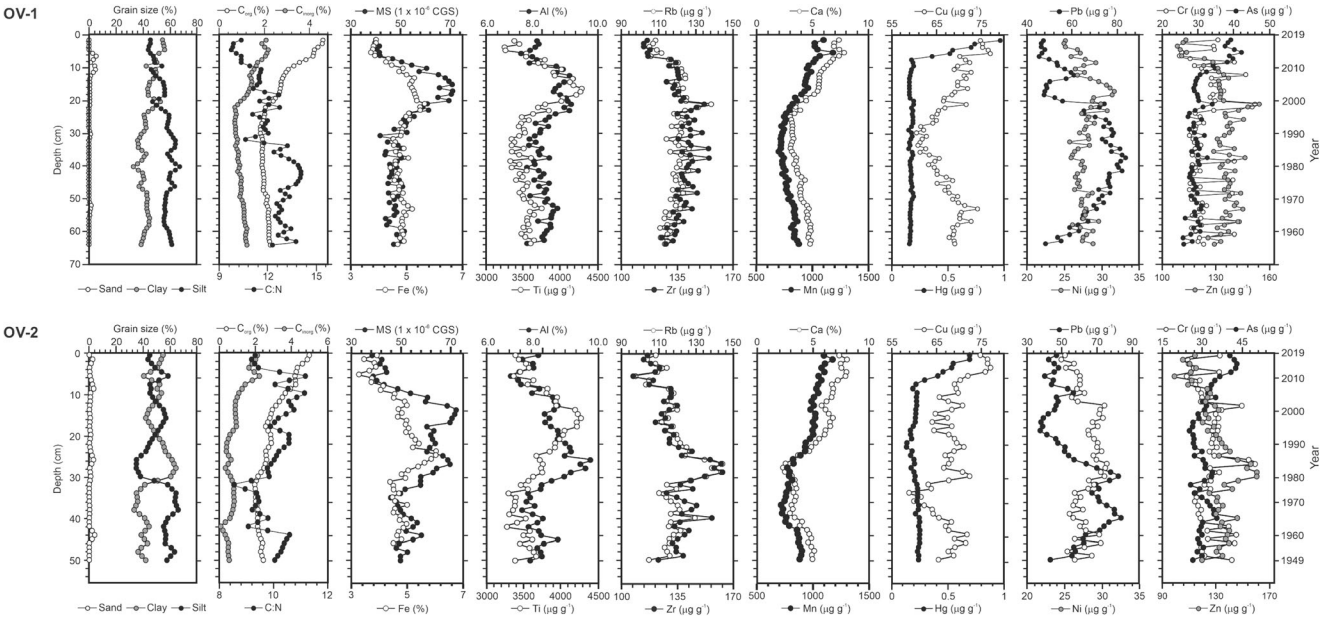

Fig. 3 Profiles of geochemical variables and trace element concentrations of sediment cores from the Oviachic reservoir, Yaqui River Basin, Northwest Mexico

and Zr were also comparable between cores. The profiles of Al, Fe, and Ti concentrations were alike in both cores, resembling those observed in the MS profiles (Fig. 3), with the highest values at subsurface sections. Rubidium and Zr concentrations increased from the core bottom up to 20–21 cm (2002) in OV-1 and from 26 to 27 cm (1991) in OV-2, and then declined upwards. In contrast, Ca and Mn concentrations decreased from the core bottom up to 23–24 (2000) in OV-1 and 23–24 cm (1995) in OV-2, and then increased steadily towards the surface.

Trace element concentrations, enrichment, and risk assessment

Trace element (As, Cr, Cu, Hg, Ni, Pb, and Zn) concentrations were similar in both cores (Table 2; Fig. 3), with almost constant distribution with depth. However, Ni, Pb, and Zn values decreased upcore, and As, Cu, and Hg maxima were observed at subsurface sections, although such increments were asynchronous (Fig. 3).

Enrichment factors (Table 2, Fig. 1S), by using pre-dam concentrations as reference values, indicated null enrichment for Cr, Cu, Ni, and Zn (EF < 1.5) along both cores; minor enrichment for As (2014–2018 in OV-1, 2015–2018 in OV-2) and Pb (1984–1996 in OV-1, 1966–1975 in OV-2). We detected a strong Hg enrichment in OV-1, and a moderate Hg enrichment in OV-2, since the early 2010s, reaching the maximum EF (5.84 for OV-1 and 3.02 for OV-2) at the core surface in both cores. The enrichment factors based on the upper continental crust concentrations (EF_{UCC}) were lower for Cr and Ni (< 1), but higher for the rest of the elements, than the enrichment factors (EF) based on pre-dam concentrations (Table 2), accounting for null enrichment for Cr and Ni concentrations, minor enrichment for Cu and Zn, minor to strong enrichment for Pb, and moderate to strong enrichment for As and Hg.

Along both cores, Cr concentrations were below the TEL value, whereas Cu, Hg, Ni, and Pb were above TEL but below PEL. Zn concentrations were above TEL in most sections, except in the uppermost segments (0–10 cm, 2012–2018, for OV-1, and 0–18 cm, 2001–2018, for OV-2). Arsenic concentrations in all of the core sections were above TEL, and above PEL in the uppermost segments (0–10 cm, 2012–2018, for OV-1, and 0–6 cm, 2014–2018, for OV-2) (Fig. 3).

Metal fluxes and flux ratios

Trace element fluxes in both cores increased with time since dam construction (mid-1950s). In OV-1, two maxima were observed (1977 and 2001), which resemble the MAR maxima. In both cores, fluxes of Pb, Ni, Cr, and Zn decreased towards the present (mostly since ~ 2000, although in OV-2 Pb fluxes decreased since ~ 1980s). Conversely, Cu, As, and Hg fluxes showed increasing values within the past 10 years (Fig. 4). Flux ratio ranges were comparable among most elements (Fig. 5, Table 2) with maxima accounting for up to ~ 4-fold increments for As, Cu, Ni, and Zn; ~ 5-fold for Cr and Pb; and ~ 15-fold increment for Hg.

Trace element provenance

We used factor analysis to assess which variables better explained the changes in trace element concentrations, and to

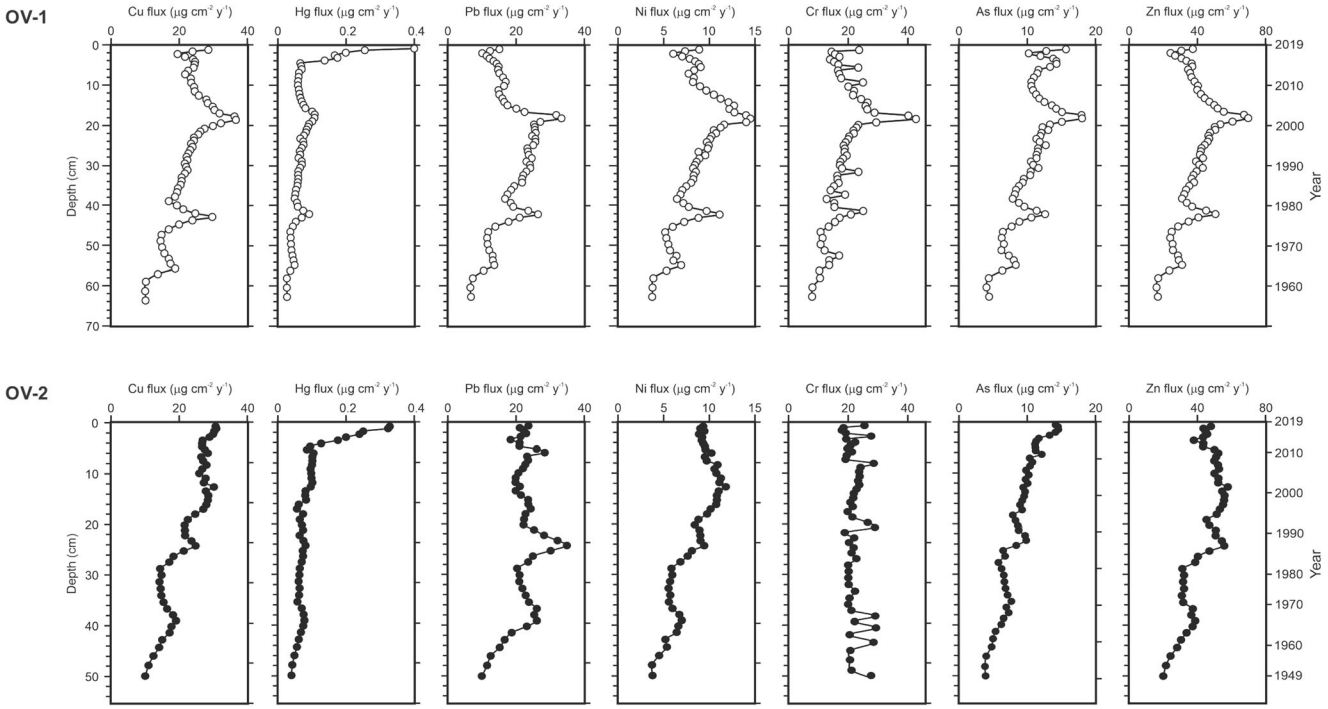

Fig. 4 Trace element fluxes in sediment cores from the Oviachic reservoir, Yaqui River Basin, Northwest Mexico

attempt elucidating their primary sources. Two factors explained ~ 70% of the dataset variability (Fig. 6, Table 3). The significant variables in factor 1 (~45% common variance) were Zn, Zr, Fe, Rb, and Pb (positive loadings) and C_{org}, Ca, Mn, C_{inorg}, Hg, As, and Cu (negative loadings). In factor 2 (25% common variance), the significant variables were silt (positive loading) and Ti, Al, clay, MS, and Ni (negative loadings).

The presence of lithophile elements in both factors, often used as indicators of terrigenous contribution (Zr, Rb, Al, and Ti; Croudace and Rothwell 2015), suggested two different terrigenous sources. Zr is an immobile element resistant to

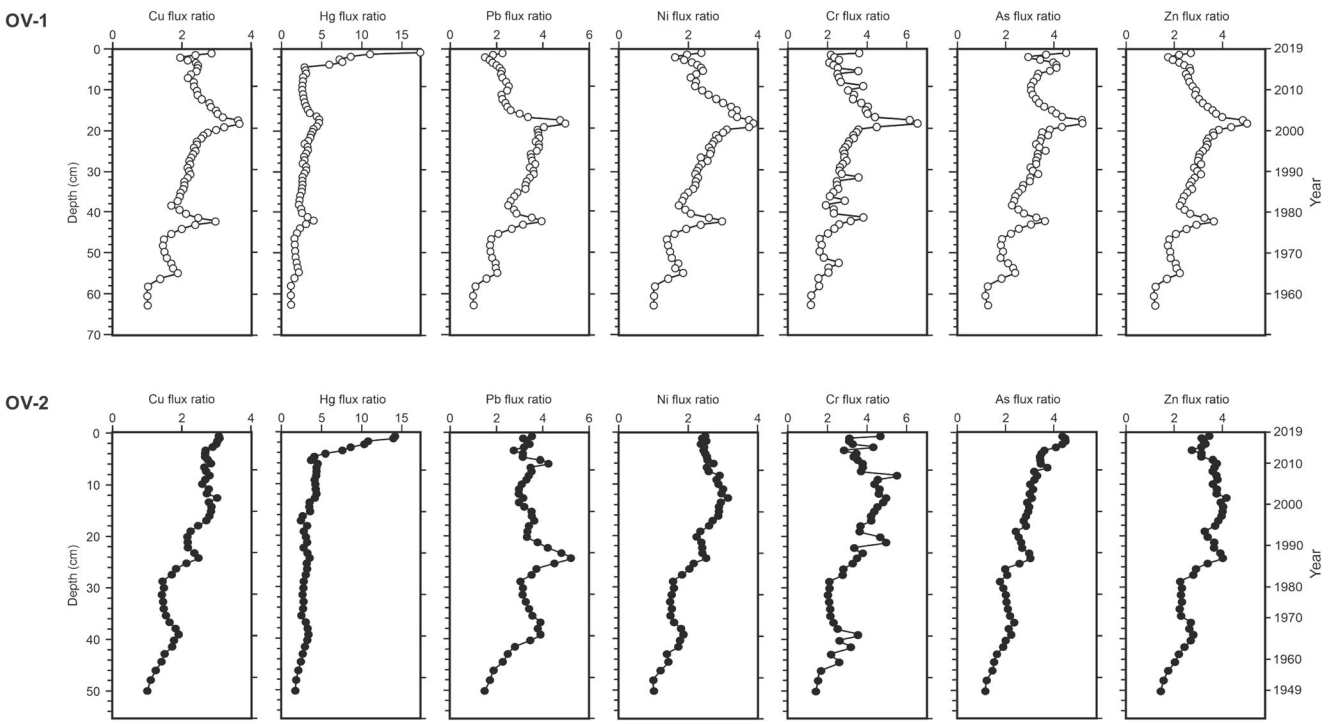

Fig. 5 Trace element flux ratios in sediment cores from the Oviachic reservoir, Yaqui River Basin, Northwest Mexico

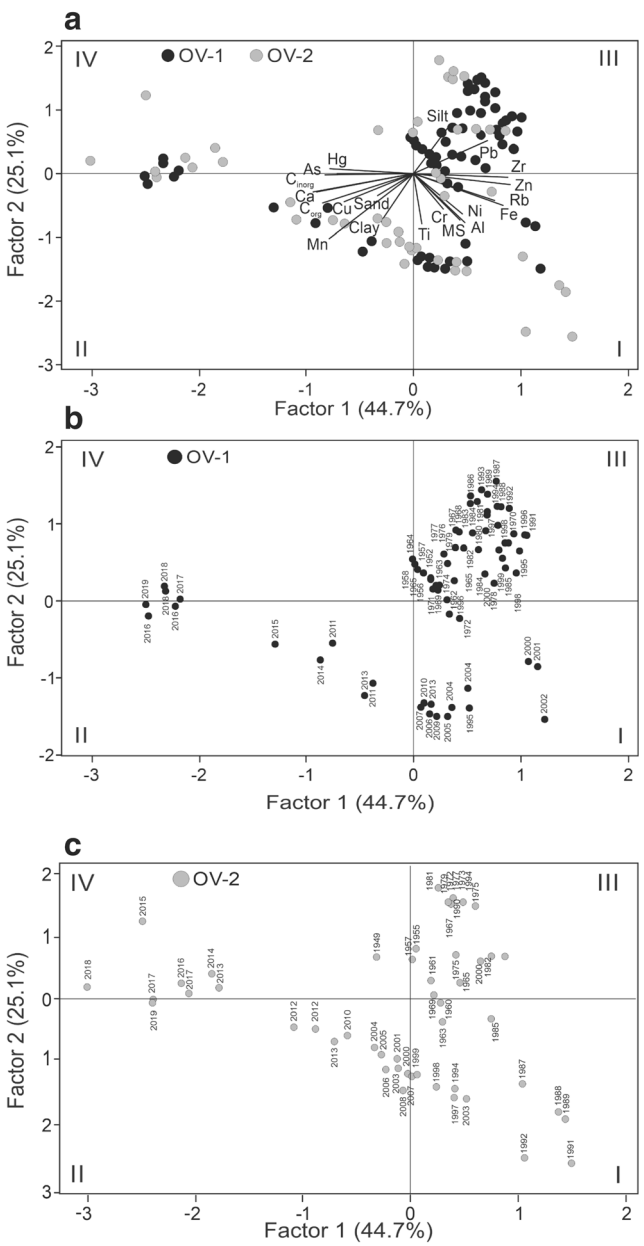

Fig. 6 Factor analysis biplot for geochemical variables and trace element concentrations in sediment cores from the Oviachic reservoir, Yaqui River Basin, Northwest Mexico. **a** Distribution of variables and observations (core sections); **b** and **c** distribution of observations per year

chemical weathering and commonly associated with detrital heavy minerals (Salminen et al. 2005), usually derived from igneous rocks, whereas Rb mostly associates with micas and K-feldspars in igneous and metamorphic rocks (Faure and Powell 1972). Al and Ti are present in many silicate minerals, such as mica, amphibole, and pyroxene, and can be enriched in weathered products of primary Al minerals such as secondary clay minerals (Salminen et al. 2005).

Thus, the presence of Zr and Rb in factor 1 accounts for the input of detrital primary minerals from the catchment. Al and Ti in factor 2 show the contribution of clay minerals in the finest sediment fraction. The significant correlations ($p < 0.05$) observed among Pb, Zn, and the lithophile elements Zr and Rb (Table 3) suggest that both trace elements have a predominant minerogenic source. The close relationship of As, Cu, and Hg with C_{org}, Ca, C_{inorg}, and Mn suggests scavenging of these trace elements by adsorption onto suspended materials (e.g., carbonates, represented by Ca and C_{inorg}), which serve as nucleation centers for the deposition of Mn hydroxides and organic coatings (Salomons and Förstner 1984) and can form strong complexes with trace elements. In summary, factor 1 accounts for the input of clastic debris and the scavenging of trace elements by suspended particles, and factor 2 accounts for the detrital contribution within fine particles (clays and silt). Ni and Cr showed non-significant loadings in both factors, as well as low, but significant ($p < 0.05$) correlations with the lithophile elements Al, Ti, Zr, and Rb, for which the main provenance of both trace elements was attributed to both detrital sources.

The distribution of the sediment sections in the loading biplot was similar for both cores (Fig. 6), showing a grouping transition: the bottom segments of the cores (between the late 1950s and 1990s) were characterized by the highest content of

Table 3 Factor analysis results for element composition in sediment cores from Oviachic reservoir, Yaqui River Basin, northwestern Mexico

Variable	Loading*		Communality
	Factor 1	Factor 2	
C_{org}	– 0.93	– 0.29	0.95
Zn	0.90	– 0.17	0.84
Ca	– 0.90	– 0.28	0.89
Zr	0.88	– 0.05	0.77
Mn	– 0.85	– 0.47	0.94
Fe	0.83	– 0.50	0.94
C_{inorg}	– 0.83	– 0.02	0.69
Hg	– 0.78	0.08	0.61
Rb	0.75	– 0.43	0.75
As	– 0.72	– 0.01	0.51
Pb	0.69	0.51	0.74
Cu	– 0.65	– 0.44	0.61
Ti	0.07	– 0.79	0.62
Al	0.47	– 0.77	0.81
Silt	0.34	0.76	0.69
Clay	– 0.30	– 0.75	0.66
MS	0.43	– 0.74	0.73
Ni	0.45	– 0.63	0.60
Cr	0.27	– 0.56	0.38
Sand	– 0.34	– 0.35	0.23
Variance+ (%)	44.7	25.1	

*Significant variables have a loading ≥ 0.65

+ Total explained variance = 69.9%

silt and Pb, as well as increasing concentrations of Rb and Sr, mostly grouped in quadrant I; the intermediate sections (between the 1990s and 2010s) were characterized by the highest values of Al and MS, mostly in quadrant II; and the uppermost sections (the 2010s) showed the highest concentrations of C_{org}, C_{inorg}, Ca, As, Hg, and Cu, and the lowest terrigenous contribution (Al, Ti, Zr, Rb, and MS), across quadrants III and IV (Fig. 6).

Discussion

^{210}Pb geochronology

$^{210}Pb_{ex}$ activity profiles in cores OV-1 and OV-2 broadly showed a decreasing trend, although some segments showed relatively constant values, which may be caused by mixing or sediment supply variability. Post-depositional mixing was considered negligible, because this process would homogenize the sediments and, consequently, other profiles (e.g., ^{137}Cs or trace elements, Figs. 2 and 3) would have shown similar patterns, which is not the case (Fig. 2). $^{210}Pb_{ex}$ activities in sediments result from the balance between the $^{210}Pb_{ex}$ flux to the sediments and sediment input (i.e., the mass accumulation rate, MAR) (Krishnaswamy et al. 1971). Consequently, $^{210}Pb_{ex}$ activities would decrease due to dilution by a higher MAR (as observed in the 23–60 cm segment of core OV-1) or increase if the MAR was lower (Sánchez-Cabeza and Ruiz-Fernández 2012). Thus, assuming that post-depositional sediment mixing is negligible, $^{210}Pb_{ex}$ activities deviating from an exponentially decreasing curve were interpreted as sediment accumulation changes. Factors influencing sediment inputs may include climate variability (the occurrence of drought or very wet periods), land use changes, and/or human-induced regulation of the water supply for flood control and land drainage.

^{137}Cs activities in both cores were comparable to or slightly lower than those reported in other continental aquatic ecosystems in Mexico, e.g., Espejo de Lirios reservoir (13.5 Bq kg^{-1}; Ruiz-Fernández et al. 2004), Zirahuén Lake (6–18 Bq kg^{-1}; Davies et al. 2004), San Marcos reservoir (7–22 Bq kg^{-1}; Méndez-García et al. 2016), and Valle de Bravo reservoir (5–20 Bq kg^{-1}; Carnero-Bravo et al. 2014), but higher than in Chapala Lake (> 1–7 Bq kg^{-1}; Ontiveros-Cuadras et al. 2014).

^{137}Cs activity profiles did not show a clear ^{137}Cs maximum that could be unequivocally attributed to the maximum ^{137}Cs fallout period (1962–1964; Robbins 1978). The highest values were observed at the deepest segment of both cores (below sections 57–58 cm in OV-1 and 45–46 cm in OV-2), and values decreased towards the present (Fig. 2). These features are compatible with the history of ^{137}Cs released to the environment in the northern hemisphere, with the onset occurring in the late 1940s (after the Trinity test in 1945), increasing fallout until a maximum in the early 1960s, and declining through the late 1960s and 1970s, after the nuclear test ban treaty went into effect in 1963 (UNSCEAR 2000). A single well-defined maximum of ^{137}Cs activity would only occur in environments where sediment accumulation was constant through the period and with a small ^{137}Cs catchment supply (Appleby et al. 2019), a condition rarely observed in aquatic ecosystems with large catchments, and impacted by land use change and soil erosion, such as the OV reservoir. Indeed, according to ^{210}Pb dating, MAR of both cores almost doubled within the period where the highest ^{137}Cs values were observed, diluting ^{137}Cs sediment activities. In addition, catchment inputs can produce a delay of the ^{137}Cs maximum, particularly in lakes with large catchments (Appleby et al. 2019), such as the OV reservoir. Furthermore, ^{137}Cs is highly mobile and can diffuse through interstitial waters, caused by ion-exchange displacement of ^{137}Cs by cations such as NH_4^+, Fe^{+2}, and Mn^{+2} released under anaerobic conditions (Evans et al. 1983), as observed in other lacustrine environments (Ligero et al. 2002; Ruiz-Fernández et al. 2004; Lan et al. 2020), disrupting the shape of the ^{137}Cs maxima. Large catchment inputs and ^{137}Cs diffusion commonly affect ^{137}Cs activity profiles from many lacustrine environments (e.g., Lan et al. 2020), which makes it difficult to corroborate ^{210}Pb age models if a single clear ^{137}Cs maximum is expected. Nonetheless, the ^{137}Cs maxima in OV cores occurred between the onset and the period of maximum global fallout from nuclear testing, which is compatible with the ^{210}Pb-derived chronology. According to the ^{210}Pb-derived age models, both cores nearly reached the pre-dam soil, as the bottom age of the cores was 1955 for OV-1 and 1949 for OV-2, which are consistent with the dam construction period (between 1947 and 1952; CONAGUA 2011).

The SAR range in OV reservoir (0.34–2.67 cm year^{-1}; Table 1, Fig. 2) was comparable to other reservoirs in Mexico, such as El Granero and San Marcos (~ 1 to > 2 cm year^{-1}; Méndez-García et al. 2016), and Intermedia and Silva (~1 cm year^{-1}; Hansen 2012). However, MAR is a better indicator to assess sedimentation processes in aquatic environments since it accounts for sediment compaction (Sánchez-Cabeza and Ruiz-Fernández 2012). MAR in OV reservoir (0.13–0.47 g cm^{-2} year^{-1}; Table 1 and Fig. 2) was similar to Espejo de Lirio Lake (0.04–0.40 g cm^{-2} year^{-1}; Ruiz-Fernández et al. 2004) and Valle de Bravo reservoir (0.12–0.40 g cm^{-2} year^{-1}; Carnero-Bravo et al. 2014), but higher than in Lago Verde Lake (0.03–0.10 g cm^{-2} year^{-1}; Ruiz-Fernández et al. 2007), Zempoala Lagoon (0.129 g cm^{-2} year^{-1}; van Afferden et al. 2005), and Miramar Lagoon (0.053 g cm^{-2} year^{-1}; Hansen 2012).

The MAR steadily increased in both cores (Fig. 2), and the most recent values, although lower than those recorded in early 2000, are 2.5-fold higher than those recorded since OV construction. These MAR increments can be caused by the progressive population growth and development of anthropogenic activities in the catchment. Dam reservoirs are fed by

erosion products of their watersheds, and as the dam building facilitates access to remote areas for new activities (e.g., road building, logging, farming, mining), they contribute to accelerated deforestation, soil loss, and sediment input to the reservoir. The Cajeme municipality, where OV is located, experienced a rapid population growth and socio-economic changes since the 1950s. The population increased almost fourfold within a decade (31,678 inhabitants in 1950 and 124,162 inhabitants in the 1960s; SE 1953; INEGI 1962) and about ~ 14 times between 1950 and 2015 (433,050 inhabitants; INEGI 2016). However, although population growth has continued to increase, MAR has decreased since the 2000s, suggesting the effect on MAR of additional factors (e.g., agriculture practices, climate variability).

Trace element concentrations, enrichment, and risk assessment

Concentrations of Ni and Zn in OV reservoir were comparable to the ranges reported for natural levels around the study area (7.09–59.3 μg g^{-1} for Ni and 66.2–107.9 μg g^{-1} for Zn; SGM 2015), but higher than those of Cu (13.7–27.3 μg g^{-1}) and Pb (14.7–35.1 μg g^{-1}) (Table 2). Besides, most element concentrations in the OV reservoir are comparable with those reported for other reservoirs in Mexico and elsewhere, affected by agriculture, urban, or industrial activities (Table 4). However, the Hg maximum is considerably higher than in all these reservoirs.

Enrichment factors were used to assess trace element contamination in OV. The short period contained in the sediment cores (~ 70 years) precluded the estimation of pre-industrial concentration levels in the area, but were useful for evaluating element enrichment since OV reservoir completion. Results indicated null enrichment by Cr, Cu, Ni, and Zn, minor enrichment by As and Pb, and strong enrichment by Hg (Fig. 1S, supplementary information). Studies elsewhere have used average shale or continental crust levels as background concentrations (e.g., Birch 2017) to estimate enrichment factors, here referred to as EF_{UCC}. In comparison with EF based on pre-dam values, EF_{UCC} indicated depletion of Cr and Ni, and different degrees of enrichment for the rest of the elements, including strong enrichment for As and Hg. However, this approach has the disadvantage that background levels do not

Table 4 Trace element concentrations (μg g^{-1}) in sediment cores from reservoirs in Mexico and elsewhere

Reservoir	Type of area	As	Cr	Cu	Hg	Ni	Pb	Zn
Oviachic reservoir (OV-1) (1)	Agricultural and mining	25.9–42.2	24.8–45.9	60.6–77.0	0.156–0.971	24.9–31.7	45.3–83.8	108.3–154.4
Oviachic reservoir (OV-2) (1)	Agricultural and mining	24.7–41.7	23.7–48.3	58.8–77.1	0.129–0.696	24.6–30.7	37.7–83.1	98.6–157.8
Intermedia reservoir, Mexico (2)	Polluted reservoir	0.6–6.8	18.8–36.7	na	0.155–0.324	8.3–36.3	7.7–25.0	38.5–134.6
Silva reservoir, Mexico (2)	Polluted reservoir	0.4–1.2	8.0–77.0	na	0.010–0.090	2.5–11.0	15.0–25.0	22.0–37.0
El Granero reservoir, Mexico (3)	Urbanized reservoir	34.0–108.5	na	na	na	na	8.4–29.7	na
San Marcos reservoir, Mexico (3)	Urbanized reservoir	15.4–32.2	na	na	na	na	39.5–83.3	na
El Tule reservoir, Mexico (4)	Agricultural activities	0.3–5.9	104–202	20.6–45.6	< 0.2	na	20.9–31.3	73.3–100.0
Chapala Lake, Mexico (4)	Urban and agricultural	6.0–9.4	43.7–57.6	23.4–28.3	0.3–1.0	na	18.8–31.0	85.1–198
Lasak reservoir, Rumania (5)	Natural reserve	8.29	28.55	22.89	0.245	14.92	<DL- 11.6	<DL- 78.5
Lochnagar Lake, Scotland (6)	Natural reserve	na	na	1.1–10.5	0.012–0.035	0.25–2.75	0.24–3.75	4.5–154
Manwan reservoir, China (7)	Urbanized reservoir	10.3–72.6	38.3–89.9	15.9–56.3	na	na	17.0–92.2	45.3–259.8
Moomaw Lake, USA (8)	Agriculture and urbanized	na	16	152	na	na	21	101
Pelham Lake, USA (8)	Agriculture and urbanized	na	46	51	na	na	19	86
Macela reservoir, Brazil (9)	Agricultural and industrialized	na	274.6	397	na	158.5	49.3	74.9
Maly Staw Lake, Poland (10)	Industrial and agricultural	na	15.4	22.9	na	6.81	176	76.5
Tisza reservoir, Hungary (11)	Industrial and mining	na	110	62	na	70	48	0.7
Pirhuacocha Lake, Peru (12)	Mining activities	na	na	26.0–170	na	na	14.0–25.1	45.0–83.5
Erhai Lake, China (13)	Mining activities	na	93–179	56–117	0.114–0.191	52–92	53–75	120–164

References: (1) this study; (2) Hansen (2012); (3) Méndez-García et al. (2016); (4) Ontiveros-Cuadras et al. (2014); (5) Begy et al. (2018); (6) Yang et al. (2002); (7) Wang et al. (2012); (8) Clark et al. (2014); (9) Santos et al. (2013); (10) Szarlowicz et al. (2018); (11) Nguyen et al. (2009); (12) Cooke et al. (2007); (13) Li et al. (2017)

na not available; *DL* detection limit

represent the specific geochemistry of the zone, which makes more uncertain the evaluation and may lead to wrong conclusions (i.e., either overestimate or underestimate enrichment), as discussed in other studies elsewhere (Rodríguez-Oroz et al. 2017; Arhin et al. 2017). This is because (1) the continental crust is composed of highly diverse lithologies, and compositional estimates may not be representative of the total continental mass (Rudnick and Gao 2004), and (2) as matter is transferred from the crust to the aquatic environment mainly via soil erosion, elements undergo natural chemical fractionation, and it is unlikely that concentrations remain constant during the biogeochemical cycle (Reimann and de Caritat 2000). Henceforward, trace element enrichment is discussed using enrichment factors based on pre-dam concentrations (EF). Despite the low enrichment, As concentrations during the last 5 years were above PEL indicating that it might cause deleterious effects on benthic biota (MacDonald et al. 2000; Buchman 2008), mainly linked to malfunction of the immune system (Duker et al. 2005).

Trace element fluxes and flux ratios

The historical metal fluxes showed increasing values since the early 1960s and high variability for most of the metals (Fig. 4). Trace element fluxes were comparable or lower than those reported for lacustrine environments, from either remote or anthropogenic-influenced areas, except for Hg, for which the maximum was considerably higher (Table 5). The long-range atmospheric transport and deposition of Hg is frequently reported around the world (Schroeder and Munthe 1998), and atmospheric deposition rates in lakes have increased during the last 20 years by a factor of 9–400 compared to background values (Biester et al. 2007). On a global scale, the major anthropogenic contribution to emissions is gold production using Hg technology (Pacyna et al. 2006). The major source of anthropogenic Hg emissions in Mexico by 1990 was nonferrous metal refining (including gold and silver refining, Pai et al. 2000). However, official data do not account for gold mining activities around Oviachic reservoir (SE 2019), and informal and unregulated mining activities (including placer-gold mining) occur at a small scale on the Yaqui River (SEMARNAT-INECC 2017).

Trace element provenance

Based on the factor analysis, Cr, Ni, Pb, and Zn delivery to the lake is predominantly terrigenous. Previous studies in Mexico and elsewhere show that Pb concentration changes in lacustrine sediments reflect the history of leaded gasoline consumption (e.g., Soto-Jiménez et al. 2006; Escobar et al. 2013). The use of tetraethyl lead in Mexico as an antiknock agent in gasoline began in the 1940s; government controls for Pb emissions started in 1982, and the phase-out of leaded gasoline was completed in 1997 (Soto-Jiménez et al. 2006). Only core OV-1 showed temporal profiles of Pb EF (Fig. 1S) and flux ratio (Fig. 5) that could be compatible with the history of Pb emissions in Mexico. However, if the direct atmospheric deposition of alkyl Pb were a significant source of Pb to the reservoir, the Pb enrichment and flux ratio profiles would be expected to show similar trends, which is not the case. The similarity of the flux ratio profiles of Cr, Ni, Pb, and Zn (Fig. 5) suggests that the input of these elements to the lake has a common source, most likely eroded soils from the catchment, which can be observed between the 1970s and 1990s in the flux ratio profiles (Fig. 5).

Erosion in the OV catchment is severe because of soil vulnerability and vegetation cover loss, attributed to overgrazing and land clearing (López-Reyes 2001), promoted by national government policies established in the 1970s to promote agricultural and livestock activities, including incentives to remove vegetation (Cedeño Gilardi and Pérez Salicrup

Table 5 Trace element fluxes (μg cm^{-2} $year^{-1}$) in sediment cores from reservoirs in Mexico and elsewhere

Reservoir	Type of area	As	Hg	Cr	Cu	Ni	Pb	Zn
Oviachic reservoir (OV-1) (1)	Agriculture, mining	0.9–4.2	1.0–14.9	0.9–5.0	1.0–3.6	1.0–3.8	1.0–4.8	1.0–4.2
Oviachic reservoir (OV-2) (1)	Agriculture, mining	1.0–3.8	0.9–7.6	0.8–3.3	0.9–2.9	1.0–3.1	0.9–3.4	1.0–2.8
Lago Verde Lake, Mexico (6)	Rural	na	0.1–6.4	na	0.2–5.2	na	0.03–2.7	0.8–9.1
Daihai Lake, China (3)	Natural reserve	na	na	na	0.2–0.8	na	0.2–1.1	na
Bang Pakong River, Thailand (2)	Industrialized	na	na	2.7	2.9	3.1	4.5	8.7
Espejo de Lirio Lake, Mexico (4)	Urbanized	na	0.03	7	1.6	na	16	13
Kamloops Lake, Canada (5)	Urbanized	na	2.5	na	na	na	1.5–4	na
Tahoe Lake, USA (8)	Urbanized	na	2.0–5.3	na	na	na	0.7–1.9	na
Lomond Lake, Scotland (7)	Industrial, urban	na	na	na	na	na	4.4	na

References: (1) this study; (2) Cheevaporn et al. (1995); (3) Han et al. (2007); (4) Ruiz-Fernández et al. (2004); (5) Gallagher et al. (2004); (6) Ruiz-Fernández et al. (2007); (7) Farmer et al. (1996); (8) Heyvaert et al. (2000)

na not available

2007). In Sonora, extensive land clearing was made for grassland cultivation to feed livestock, especially Buffelgrass (*Cenchrus ciliaris* L.), the extension of which increased from 1000 ha in the 1970s to 400,000 ha in the late 1980s (López-Reyes 2001). Buffelgrass erosion rates are positively correlated with plant densities, owing to inefficient pasture management, i.e., overgrazing (Valdez-Zamudio and Guertin 2000). The reduction of Cr, Ni, Pb, and Zn fluxes since the 2000s may also be associated with government policies related to the implementation of control measures on land use change from forest to agricultural lands (DOF 1994), the deterioration of the agro-livestock sector as a consequence of unfavorable economic conditions, and the growth of the industrial sector in Sonora (COESPO 2010), but also likely with climate variability and water scarcity.

An increasing trend in atmospheric temperature has been reported for the lower basin of Yaqui River within the past 4 decades (Martínez-Austria et al. 2014), and since the late 1990s, its watershed has experienced strong drought conditions. Since then, the average annual runoff is below the historical mean (3061 hm^3 per year; Minjares-Lugo and Salomón-Castelo 2009), causing the reservoir system, including OV, to attain the lowest historical level in 2004, with only ~ 13% of the storage capacity (Cortés-Jiménez et al. 2009). Rainfall reduction not only affects river runoff but also reduces the efficiency of the aquifer recharge from surface runoff infiltration, which can affect the height of the water table, the concentration of trace elements in groundwater, and the concentration of dissolved constituents (major ions and trace elements) in the reservoir waters.

Reduced rainfall may explain the highest concentrations observed since the early 2000s for Mn, carbonates (C_{inorg} and Ca), and C_{org}, and the fluxes and flux ratios of As and Cu, because of the concentration enhancement of these constituents, either in the aquifer waters or within the reservoir. Little is known about the three aquifers discharging into OV, except that (a) they are an unconfined type with shallow phreatic levels, formed by a sequence of coarse grain alluvial deposits with high permeability (restricted to the channels of streams with reduced thickness), and below this sequence and outside the channels of rivers and streams, the aquifer is made up of conglomerates, volcanic and intrusive rocks that present secondary permeability due to fracturing; (b) the main source of recharge is rainfall infiltration from surface runoff; (c) the area where they transit is rural (with scarce seasonal agriculture and cattle raising) without urban/industrial centers; (d) they are underexploited; and (e) the water quality is adequate for human consumption (low total dissolved solids and electric conductivity, high dissolved oxygen concentrations, and circumneutral pH), although it is not ruled out that major ions and/or heavy metals in high concentrations could result from water-rock interaction during groundwater transition associated with longer residence times and transit of water in the aquifer (CONAGUA 2015).

Despite the mining activities in the region, As and Cu in OV sediments are mostly of natural origin (as indicated by the low EF), most likely the result of weathering in the catchment and water-rock interaction within the aquifers draining to the reservoir. Strongly reducing aquifers derived from alluvium or loess, or inland aquifers in arid or semi-arid environments (such as this case), may have high As concentrations, often in combination with Mn and other trace elements, especially when groundwater movement is slow and there is element bedrock enrichment, which allows the accumulation rather than flushing of toxic metals (Mitchell et al. 2012). Although we lack information on trace element concentrations of the water delivered to OV reservoir, it is likely that lower recharge of the aquifers

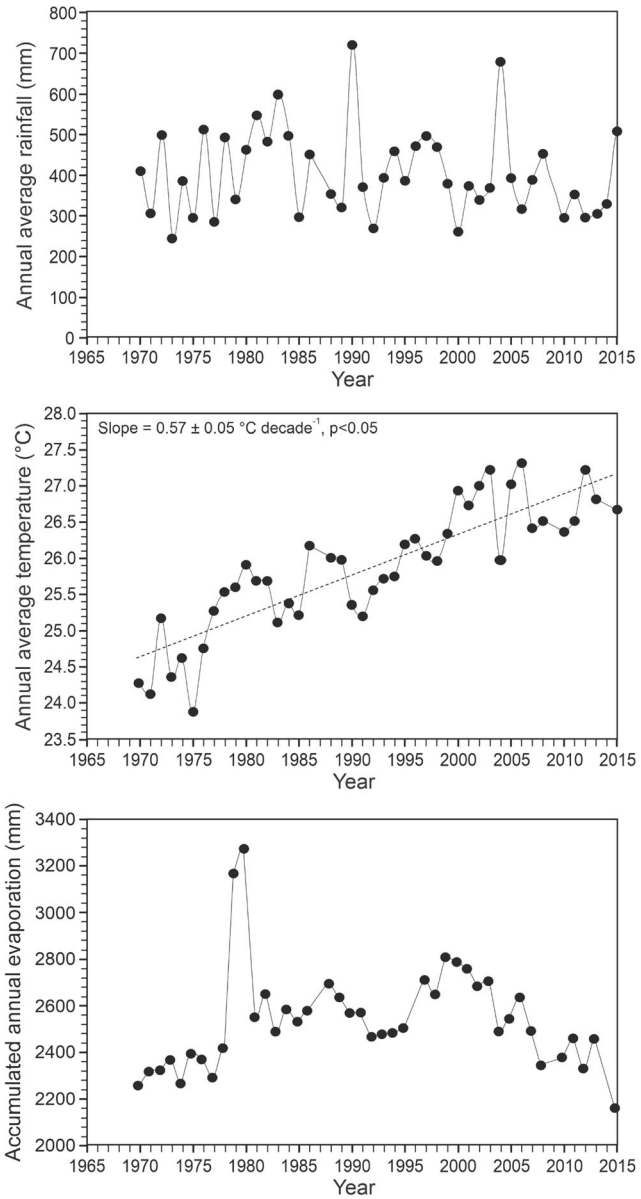

Fig. 7 Annual variations in precipitation, temperature, and evaporation at the Oviachic reservoir, Yaqui River Basin, Northwest Mexico

draining to OV reservoir caused by lower rainfall has promoted the delivery of water with higher concentrations of As, Cu, Mn, and carbonates.

According to the meteorological records in OV (CONAGUA 2020a), the mean annual temperature between 1970 and 2015 has increased by ~ 0.6 °C decade^{-1} and, although the rainfall record is very irregular, since 1985, most maxima have been considerably lower than those of the previous years (Fig. 7). Evaporation within the reservoir has increased as a result of higher temperatures and low rainfall, promoting higher authigenic carbonate precipitation. All trace element flux ratios presented two maxima around 1977 and 2000 (most evident in OV-2; Figs. 3 and 4), which correspond to the lowest rainfall (285 mm during 1977 and 261 mm during 2000; CONAGUA 2020b). This may be related to excessive evaporation and continuous precipitation of metals during that period.

Although Hg has a significant correlation with As and Cu (most likely owing to scavenging, common for the three elements), the timing and shape of the Hg flux profiles are different, and EFs and flux ratios are higher for Hg (Figs. 4 and 5) than for As and Cu, suggesting an additional anthropogenic source. This additional Hg source is most likely related with the relatively recent proliferation of small-scale artisanal gold mining activities, which use mercury as amalgamator, across the Yaqui River Basin (personal communications from locals; SEMARNAT-INECC 2017). Local newspapers report that Sonora is experiencing a "new gold rush" caused by the availability of gold resources and current high gold prices. In addition, there are environmental authority reports since 2010 informing about the suspension of activities and imposition of fines to irregular mining areas, some of them on the north of the OV reservoir, along the Yaqui River banks (e.g., PROFEPA 2010).

Conclusions

The reconstruction of temporal changes in sedimentation rates and trace element (As, Cr, Cu, Hg, Ni, Pb, and Zn) enrichment and fluxes, as recorded in two ^{210}Pb-dated sediment cores from Oviachic reservoir, showed that the sediment load has increased steadily over the past 70 years (currently ~ 2.5 times higher than when the reservoir was completed) and that trace element contamination is mostly minimal, except for Hg. Nonetheless, according to international guidelines, some of the As, Cu, Pb, and Hg concentrations could be noxious for the benthic biota (and humans, through fish consumption). Highest Cr, Ni, Pb, and Zn fluxes, recorded between the 1970s and the 1990s, were attributed to soil erosion in the watershed, promoted by inadequate agriculture and husbandry practices. The recent increasing fluxes, observed within the past decade for As and Cu, are likely triggered by dryer climate conditions, enhancing concentrations either by lower rainfall and aquifer recharge, or water evaporation in the reservoir; whereas for Hg, the input of wastes from artisanal-scale gold mining activities (which use Hg as amalgamator) is suspected. Further studies on artisanal gold mining affecting the Yaqui River and the OV dam by Hg input are urgently needed and, if confirmed, regulations should be developed and implemented. Additionally, a human health risk assessment following exposure to Hg in water and fish consumption from the OV dam is strongly recommended. This study provides baseline data useful for further research on anthropogenic and climate impacts in reservoirs in the region. It highlights the importance of conducting specific risk assessments in lacustrine environments where fish production is relevant for human consumption and as a livelihood, and where water is used for public supply.

Supplementary Information The online version contains supplementary material available at https://doi.org/10.1007/s11356-020-11995-3.

Acknowledgments This study was supported by the project grant # 20562 "Accumulation and distribution of metals and metalloids in water, sediments and biota in the Yaqui River Basin, Sonora State," from Centro de Investigación en Alimentación y Desarrollo, A.C. The scholarship of R. Ochoa-Contreras was provided by the Consejo Nacional de Ciencia y Tecnología of México. The authors are grateful to Adolfo Americano for the technical assistance during sampling activities and to Germán Ramírez, Carlos Suárez, and León Felipe Álvarez for the data curation and processing.

Authors' contributions Jara-Marini M.E., Ruiz-Fernández A.C., and Sanchez-Cabeza J.A. contributed to the study conception and design. Material preparation, data collection, and analysis were performed by Ochoa-Contreras R., Pérez-Bernal L.H., Meza-Figueroa D.M., Ruiz-Fernández A.C., Jara-Marini M.E., and Sanchez-Cabeza J.A. The first draft of the manuscript was written by Ochoa-Contreras R. and Ruiz-Fernández A.C. All authors commented on previous versions of the manuscript. All authors read and approved the final manuscript.

Funding Financial support was received from Centro de Investigación en Alimentación y Desarrollo, A.C., under grant agreement # 20562. Consejo Nacional de Ciencia y Tecnología of México provided the PhD scholarship of R. Ochoa-Contreras.

Data availability The datasets used and/or analyzed during the current study are available from the corresponding author on reasonable request.

Compliance with ethical standards

Conflict of interest The authors declare that they have no conflict of interest.

Ethics approval and consent to participate Not applicable

Consent for publication Not applicable

References

Adler T (2005) The arsenic differential: metabolism varies between children and adults. Environ Health Perspect 113(6):A404

Appenroth K (2010) Definition of "heavy metals" and their role in biological systems. In: Sherameti I, Varma A (eds) Soil heavy metals, soil biology. Springer-Verlag, Berlin Heidelberg, pp 19–29. https://doi.org/10.1007/978-3-642-02436-8_2

Appleby PG (1998) Dating recent sediments by 210 Pb: problems and solutions (STUK-A–145). Illus, E. (Ed.). Finland

Appleby PG, Semertzidou P, Piliposian GT, Chiverrell RC, Schillereff DN, Warburton J (2019) The transport and mass balance of fallout radionuclides in Brotherswater, Cumbria (UK). J Paleolimnol 62: 389–407

Arhin E, Mouri H, Kazapoe R (2017) Inherent errors in using continental crustal averages and legislated accepted values in the determination of enrichment factors (EFs): A case study in northern Ghana in developing environmental policies. J Geogr Nat Disast 7:204. https://doi.org/10.4172/2167-0587.1000204

Begy RC, Kelemen S, Simon H, Tănăselia C (2018) The history of the sedimentation processes and heavy metal pollution in the central Danube delta (Romania). Geochronometria. 45:97–106. https://doi.org/10.1515/geochr-2015-0090

Berner RA (1964) An idealized model of dissolved sulfate distribution in recent sediments. Geochim Cosmochim Acta 28(9):1497–1503. https://doi.org/10.1016/0016-7037(64)90164-4

Biester H, Bindler R, Martinez-Cortizas A, Engstrom DR (2007) Modeling the past atmospheric deposition of mercury using natural archives. Environ Sci Technol 41(14):4851–4860. https://doi.org/10.1021/es0704232

Birch GF (2017) Determination of sediment metal background concentrations and enrichment in marine environments - a critical review. Sci Total Environ 580:813–831. https://doi.org/10.1016/j.scitotenv.2016.12.028

Buat-Menard P, Chesselet R (1979) Variable influence of the atmospheric flux on the trace-metal chemistry of oceanic suspended matter. Earth Planet Sci Lett 42(3):399–411. https://doi.org/10.1016/0012-821X(79)90049-9

Buchman MF (2008) NOAA screening quick reference tables (SQuiRTs). NOAA OR&R Report 08-1. National Oceanic and Atmospheric Administration. 34 pp

Cantú-Soto EU, Harris R, Roberge J, Klimecki WT, Félix-Fuentes A, Meza-Montenegro MM (2009) Determinación de polimorfismos del gen Arsénico 3 Metiltransferasa (As3MT) asociado al metabolismo del arsénico, en la población del valle del Yaqui, Sonora, México. Rev Latinoam Recurs Nat 5(2):155–160

Carnero-Bravo V, Merino-Ibarra M, Ruiz-Fernández AC, Sanchez-Cabeza J, Ghaleb B (2014) Sedimentary record of wáter column trophic conditions and sediment carbon fluxes in a tropical water reservoir (Valle de Bravo, Mexico). Environ Sci Pollut Res 22: 4680–4694. https://doi.org/10.1007/s11356-014-3703-0

Cedeño Gilardi H, Pérez Salicrup DR (2007) La legislación forestal y su efecto en la restauración de México. Instituto Nacional de Ecología y Cambio Climatico. Centro de Investigaciones en Ecosistemas, Universidad Nacional Autónoma de México. Sanchez O. (ed). pp. 87 - 97

Cheevaporn V, Jacinto GS, San Diego-McGlone ML (1995) Heavy metal fluxes in Bang Pakong River estuary, Thailand: sedimentary vs diffusive fluxes. Mar Pollut Bull 31(4-12):290–294. https://doi.org/10.1016/0025-326X(95)00195-S

Child D (2006) The essentials of factor analysis, 3rd edn. Continuum International Publishing Group, Bodmin, p 180

Ciszewski D, Grygar TM (2016) A review of flood-related storage and remobilization of heavy metal pollutants in river systems. Water Air Soil Pollut 227:239. https://doi.org/10.1007/s11270-016-2934-8

Clark EV, Odhiambo BK, Ricker MC (2014) Comparative analysis of metal concentrations and sediment accumulation rates in two Virginian reservoirs, USA: lakes Moomaw and Pelham. Water Air Soil Pollut 225:1860. https://doi.org/10.1007/s11270-013-1860-2

COESPO (2010) 100 Años de Población y Desarrollo. Consejo Estatal de Población de Sonora. Tomo II Periodo 1950-2000. 290 pp (in Spanish)

CONAGUA (2008) Comisión Nacional del Agua, Secretaría de Medio Ambiente y Recursos Naturales, ed. Estadísticas del Agua en México - Edición 2008. pp 69. ISBN 978-968-817-895-9 (in Spanish)

CONAGUA (2011) Comisión Nacional del Agua, Memoria descriptiva de la presa Álvaro Obregón (El Oviachic). Subgerencia de Seguridad de Presas. 12 pp (in Spanish)

CONAGUA (2015) Disponibilidad por acuíferos-Sonora. Comisión Nacional del Agua (in Spanish). (Accessed in Jun 2020)

CONAGUA (2018) Estadísticas del agua en México. Comisión Nacional del Agua. Secretaría del Medio Ambiente y Recursos Naturales. Ciudad de México. 303 pp (in Spanish)

CONAGUA (2020a) Comisión Nacional del Agua, Sistema Nacional de Información del Agua. Monitoreo de las Principales Presas de México (in Spanish). http://sina.conagua.gob.mx/sina/almacenamientoPresas.php (Accessed in Apr 2020)

CONAGUA (2020b) Comisión Nacional del Agua, Servicio Meteorológico Nacional. Normales Climatológicas por Estado (in Spanish). https://smn.conagua.gob.mx/tools/RESOURCES/Mensuales/son/00026068.TXT (Accessed in Jun 2020)

Cooke CA, Abbott MB, Wolfe AP, Kittleson JL (2007) A millennium of metallurgy recorded by lake sediments from Morococha, Peruvian Andes. Environ Sci Technol 41:3469–3474. https://doi.org/10.1021/es062930

Cortés-Jiménez JM, Troyo-Diéguez E, Murillo-Amador B, García-Hernández JL, Garatuza-Payán J, Suh Lee S (2009) Índices de la calidad del agua del acuífero del Valle del Yaqui, Sonora. Terra Latinoamericana 27(2):133–141 (in Spanish)

Croudace IW, Rothwell RG (2015) Micro-XRF studies of sediment cores. Application of a non-destructive tool for the environmental sciences. Developments in Paleoenvironmental Research. 655 pp. ISBN: 978-94-017-9849-5

Davies SJ, Metcalfe SE, MacKenzie AB, Newton AJ, Endfield GH, Farmer JG (2004) Environmental changes in the Zirahuén Basin, Michoacán, México, during the last 1000 years. J Paleolimnol 31: 77–98. https://doi.org/10.1023/B:JOPL.0000013284.21726.3d

De la O-Villanueva M, Meza-Figueroa D, Maier RM, Moreno D, Gómez-Alvarez A, Del Río-Salas R, Mendivil H, Montijo A (2013) Procesos erosivos en jales de la Presa I de Nacozari de García, Sonora y su efecto en la dispersión de contaminantes. B Soc Geol Mex 65(1):27–38

Díaz-Asencio M, Sanchez-Cabeza JA, Ruiz-Fernández AC, Corcho-Alvarado JA, Pérez-Bernal LH (2020) Calibration and use of well-type germanium detectors for low-level gamma-ray spectrometry of sediments using a semi-empirical method. J Environ Radioact 225: 106385. https://doi.org/10.1016/j.jenvrad.2020.106385

DOF (1994) NORMA Oficial Mexicana NOM-062-ECOL-1994, que establece las especificaciones para mitigar los efectos adversos sobre la biodiversidad que se ocasionen por el cambio de uso del suelo de terrenos forestales a agropecuarios. Diario Oficial de la Federación, 13/05/1994

Duker AA, Carranza EJM, Hale M (2005) Arsenic geochemistry and health. Environ Int 31(5):631–641. https://doi.org/10.1016/j.envint.2004.10.020

Enríquez D, Durán G (2017) Las grandes presas en el río Yaqui (Sonora, México) y sus efectos socio-ambientales. Antropol Sociol 19:165–188. https://doi.org/10.17151/rasv.2017.19.1.9

Escobar J, Whitmore TJ, Kamenov GD, Riedinger-Whitmore MA (2013) Isotope record of anthropogenic lead pollution in lake sediments of Florida, USA. J Paleolimnol 49:237–252. https://doi.org/10.1007/s10933-012-9671-9

Essien JP, Antai SP, Olajire AA (2009) Distribution, seasonal variations and ecotoxicological significance of heavy metals in sediments of

cross river estuary mangrove swamp. Water Air Soil Pollut 197:91–105. https://doi.org/10.1007/s11270-008-9793-x

Evans DW, Alberts JJ, Clark RA III (1983) Reversible ion-exchange fixation of cesium-137 leading to mobilization from reservoir sediments. Geochim Cosmochim 41:1041–1049

Farmer JG, Eades LJ, Mackenzie AB, Kirika A, Bailey-Watts TE (1996) Stable lead isotope record of lead pollution in Loch Lomond sediments since 1630 A.D. Environ Sci Technol 30:3080–3083. https://doi.org/10.1021/es960162o

Faure G, Powell JL (1972) Strontium Isotope Geology. Springer-Verlag, Berlin, p 188

Gallagher L, MacDonald RW, Paton DW (2004) The historical record of metals in sediments from six lakes in the Fraser river basin, British Columbia. Water Air Soil Pollut 152:257–278. https://doi.org/10.1023/B:WATE.0000015349.25371.af

Garrido-Hoyos (2019) Estimación y dispersión de contaminantes en el río Yaqui (Sonora, México); evaluación y riesgos ambientales. Coordinación de desarrollo profesional e institucional, Subcoordinación de posgrado. Instituto Mexicano de Tecnología del Agua, 240 pp (in Spanish)

Guillette EA, Meza MM, Aquilar MG, Soto AD, Garcia IE (1998) An anthropological approach to the evaluation of preschool children exposed to pesticides in Mexico. Environ Health Perspect 106(6): 347–353. https://doi.org/10.1289/ehp.98106347

Han Y, Jin Z, Cao J, Posmentier ES, An Z (2007) Atmospheric Cu and Pb deposition and transport in lake sediments in a remote mountain area, northern China. Water Air Soil Pollut 179:167–181. https://doi.org/10.1007/s11270-006-9222-y

Hansen AM (2012) Lake sediment cores as indicators of historical metal(loid) accumulation - a case study in Mexico. J Appl Geochem 27: 1745–1752. https://doi.org/10.1016/j.apgeochem.2012.02.010

Heyvaert AC, Reuter JE, Slotton DG, Goldman CR (2000) Historical atmospheric lead and mercury deposition at Lake Tahoe, California-Nevada. Environ Sci Technol 34(17):3588–3597. https://doi.org/10.1021/es991309p

INAFED (2019) Enciclopedia de Los Municipios y Delegaciones de México Estado de Sonora. Cajeme. Instituto Nacional para el Federalismo y el Desarrollo Municipal (in Spanish). http://www.inafed.gob.mx/work/enciclopedia/EMM26sonora/municipios/26018a.html (Accessed in Jun 2020)

INEGI (1962) Octavo censo general de población - 1960: 8 de Junio de 1960. Secretaría de Industria y Comercio, Dirección general de estadística. pp 710

INEGI (2000) Síntesis de Información Geográfica del Estado de Sonora. Hidrología. Instituto Nacional de Estadistica, Geografía e Informática. 10 pp (in Spanish)

INEGI (2016) Panorama sociodemográfico de Sonora 2015. Instituto Nacional de Estadística y Geografía. pp. 169 (in Spanish)

INEGI (2017) Anuario estadístico y geográfico de Sonora 2017. Instituto Nacional de Estadística y Geografía. 672 pp (in Spanish). https://www.datatur.sectur.gob.mx/ITxEF_Docs/SON_ANUARIO_PDF.pdf (Accessed in Dec 2019).

INEGI (2018) Anuario estadístico y geográfico de Sonora 2018. Instituto Nacional de Estadística y Geografía. pp. 639

Krishnamurty KV, Shpirt E, Reddy MM (1976) Trace metal extraction of soil and sediments by nitric acid-hydrogen peroxide. Atom Absorpt Newsl 15(3):68–70

Krishnaswamy S, Lal D, Martin J, Meybeck M (1971) Geochronology of lake sediments. Earth Planet Sci Lett 11:407–414

Kuselman I, Fajgelj A (2010) IUPAC/CITAC guide: selection and use of proficiency testing schemes for a limited number of participants-chemical analytical laboratories (IUPAC Technical Report). Pure Appl Chem 82(5):1099–1135. https://doi.org/10.1351/PAC-REP-09-08-15

Lan J, Wang T, Chawchai S, Cheng P, Zhou K, Yu K, Yan D, Wang Y, Zang J, Liu Y, Tan L, Ai L, Xu H (2020) Time marker of 137Cs fallout maximum in lake sediments of Northwest China. Quat Sci Rev 241:106413. https://doi.org/10.1016/j.quascirev.2020.106413

Li K, Liu E, Zhang E, Li Y, Shen J, Liu X (2017) Historical variations of atmospheric trace metal pollution in southwest China: reconstruction from a 150-years lacustrine sediment record in the Erhai Lake. J Geochem Explor 172:62–70. https://doi.org/10.1016/j.gexplo.2016.10.009

Ligero RA, Barrera M, Casas-Ruiz M, Sales D, López-Aguayo F (2002) Dating of marine sediments and time evolution of heavy metal concentrations in the Bay of Cádiz, Spain. Environ Pollut 118:97–108. https://doi.org/10.1016/s0269-7491(01)00209-3

López-Reyes M (2001) Degradación de suelo en Sonora: el problema de la erosión en los suelos de uso ganadero. El Colegio de Sonora, Región y Sociedad 13(22):73–97

Loring DH, Rantala RTT (1992) Manual for the geochemical analyses of marine sediments and suspended particulate matter. Earth Sci Rev 32(4):235–283. https://doi.org/10.1016/0012-8252(92)90001-A

MacDonald DD, Ingersoll CG, Berger TA (2000) Development and evaluation of consensus-based sediment quality guidelines for freshwater ecosystems. Arch Environ Contam Toxicol 39:20–31. https://doi.org/10.1007/s002440010075

Martínez-Austria PF, Patiño-Gómez C, Tamayo-Escobar JE (2014) Análisis de tendencias climáticas en la cuenca baja del río Yaqui, Sonora, México. Technol Cienc Agua 5(6):135–149

Méndez-García CG, Luna-Porres MY, Montero-Cabrera ME, Renteria-Villalobos M, Pérez-Cázares B, García-Tenorio R (2016) Arsenic, lead, and uranium concentrations on sediments deposited in reservoirs in the Rio Grande Basin, USA-Mexico border. J Soils Sediments 16:1970–1985. https://doi.org/10.1007/s11368-016-1400-y

Meza-Figueroa D, Maier RM, De la O-Villanueva M, Gómez-Alvarez A, Moreno-Zazueta A, Rivera J, Campillo A, Grandlic C, Anaya R, Palafox-Reyes J (2009) The impact of unconfined mine tailings in residential areas from a mining town in a semi-arid environment: Nacozari, Sonora, Mexico. Chemosphere. 77(1):140–147. https://doi.org/10.1016/j.chemosphere.2009.04.068

Meza-Montenegro MM, Gandolfi AJ, Santana-Alcántar ME, Klimecki WT, Aguirlar-Apodaca MG, Del Río-Salas R, De la O-Villanueva M, Gómez-Alvarez A, Mendivil-Quijada H, Valencia M, Meza-Figueroa D (2012) Metals in residential soils and cumulative risk assessment in Yaqui and Mayo agricultural valleys, northern Mexico. Sci Total Environ 657:1468–1479. https://doi.org/10.1016/j.scitotenv.2012.06.083

Minjares-Lugo JL, Salomón-Castelo RF (2009) Índice económico para el manejo interanual del agua: caso del Distrito de Riego 041 Río Yaqui, México. Ingeniería hidráulica en México 24(1):41–54

Mishra S, Bharagava RN, Yadav A, Zainith S, Chowdhary P (2019) Heavy metal contamination: an alarming threat to environment and human health. In: Sobti RC, Arora NK, Kothari R (eds) Environmental biotechnology: for sustainable future. Springer Nature Singapore Pte Ltd., Singapore, pp 104–119. https://doi.org/10.1007/978-981-10-7284-0_5

Mitchell PJ, Lane PNJ, Benyon RG (2012) Capturing within catchment variation in evapotranspiration from montane forests using LiDAR canopy profiles with measured and modelled fluxes of water. Ecohydrol. 5:708–720. https://doi.org/10.1002/eco.255

Muñoz-Arriola F, Avissar R, Zhu C, Lettenmaier DP (2009) Sensitivity of water resources of Rio Yaqui Basin, Mexico, to agricultural extensification under multiscale climate conditions. Water Resour Res 45:1–19. https://doi.org/10.1029/2007WR006783

Nguyen HL, Braun M, Szaloki I, Baeyens W, Van Grieken R, Leermakers M (2009) Tracing the metal pollution history of the

Tisza River through the analysis of a sediment depth profile. Water Air Soil Pollut 200:119–132. https://doi.org/10.1007/s11270-008-9898-2

Ontiveros-Cuadras JF, Ruiz-Fernández AC, Sanchez-Cabeza JA, Pérez-Bernal LH, Sericiano JL, Preda M, Liong Wee Kwong L, Páez-Osuna F (2014) Trace element fluxes and natural potential risks from 210Pb-dated sediment cores in lacustrine environments at the Central Mexican Plateau. Sci Total Environ 468-469:677–687. https://doi.org/10.1016/j.scitotenv.2013.08.071

Pacyna E, Pacyna J, Fudala J, Strzelecka-Jastrzab E, Hlawiczka S, Panasiuk D (2006) Mercury emissions to the atmosphere from anthropogenic sources in Europe in 2000 and their scenarios until 2020. Sci Total Environ 370:147–156. https://doi.org/10.1016/j.scitotenv.2006.06.023

Pai P, Niemi D, Powers B (2000) A North American inventory of anthropogenic mercury emissions. Fuel Process Technol 65-66:101–115. https://doi.org/10.1016/S0378-3820(99)00079-X

Peters K, Bundschuh M, Schafer RB (2013) Review on the effects of toxicants on freshwater ecosystem functions. Environ Pollut 180: 324–329. https://doi.org/10.1016/j.envpol.2013.05.025

PROFEPA (2010). Clausura PROFEPA mina de oro de placer en Sonora. Procuraduría Federal de Protección al Ambiente. Mexico. https://www.profepa.gob.mx/innovaportal/v/5989/1/mx.wap/clausura_profepa_mina_de_oro_de_placer_en_sonora.html. Accessed Sept 2020.

Qi S, Leipe T, Rueckert P, Di Z, Harff J (2010) Geochemical sources, deposition and enrichment of heavy metals in short sediment cores from the Pearl River estuary, southern China. J Mar Syst 82:S28–S42. https://doi.org/10.1016/j.jmarsys.2010.02.003

Reimann C, de Caritat P (2000) Intrinsic flaws of element enrichment factors (EFs) in environmental geochemistry. Environ Sci Technol 34(24):5084–5091. https://doi.org/10.1021/es001339o

Reza R, Singh G (2010) Heavy metal contamination and its indexing approach for river water. Int J Environ Sci Technol 7:785–792. https://doi.org/10.1007/BF03326187

Robbins JA (1978) Geochemical and geophysical applications of radioactive lead. In: Nriagu JO (ed) Biogeochemistry of lead in the environment. Elsevier Scientific, Amsterdam, pp 285–393

Rodríguez-Oroz D, Lasheras E, Elustondo D, Garrigó (2017) Assessment of indexes for heavy metal contamination in remote areas: a case study in a Pyrenean forest, Navarra, Spain. Bull Environ Contam Toxicol 98:91–96. https://doi.org/10.1007/s00128-016-1972-7

Rudnick RL, Gao S (2004) Composition of the continental crust. In: Hollands HD, Turekian KC (eds) Treatise on geochemistry 3. Elsevier, Amsterdam, 64 pp. https://doi.org/10.1016/B0-08-043751-6/03016-4

Ruiz-Fernández AC, Hillaire-Marcel C (2009) 210Pb-derived ages for the reconstruction of terrestrial contaminant history into the Mexican Pacific coast: potential and limitations. Mar Pollut Bull 59(4-7):134–145. https://doi.org/10.1016/j.marpolbul.2009.05.006

Ruiz-Fernández AC, Páez-Osuna F, Urrutia-Fucugauchi J, Preda M, Rehault I (2004) Historical trace metal fluxes in the Mexico City Metropolitan Zone as evidence by a sedimentary record from the Espejo de los Lirios lake. J Environ Monit 6:473–480. https://doi.org/10.1039/b316583c

Ruiz-Fernández AC, Páez-Osuna F, Urrutia-Fucugauchi J, Preda M (2005) ^{210}Pb geochronology of sediment accumulation rates in México City Metropolitan Zone as recorded at Espejo de los Lirios lake sediments. Catena. 61:31–48. https://doi.org/10.1016/j.catena.2005.01.003

Ruiz-Fernández AC, Hillaire-Marcel C, Páez-Osuna F, Ghaleb B, Caballero M (2007) 210Pb chronology and trace metal geochemistry at Los Tuxtlas, Mexico, as evidenced by a sedimentary record from the Lago Verde crater lake. Quat Res 67:181–192. https://doi.org/10.1016/j.yqres.2006.11.003

Ruiz-Fernández AC, Ontiveros-Cuadras JF, Sericano JL, Sánchez-Cabeza JA, Wee Kwong LL, Dunbar RB, Mucciarone DA, Pérez-Bernal LH, Páez-Osuna F (2014) Long-range atmospheric transport of persistent organic pollutants to remote lacustrine environments. Sci Total Environ 493:505–520. https://doi.org/10.1016/j.scitotenv.2014.05.002

Salminen R, Reeder S, De Vivo B, Demetriades A, Pirc S, Batista MJ, Marsina K, Ottesen RT, O'Connor PJ, Bidovec M, Lima A, Siewers U, Smith B, Taylor H, Shaw R, Salpeteur I, Gregorauskiene V, Halamic J, Slaninka I, Lax K, Gravesen P, Birke M, Breward N, Ander EL, Jordan G, Duris M, Klein P, Locutura J, Bel-lan A, Pasieczna A, Lis J, Mazreku A, Gilucis A, Heitzmann P, Klaver G, Petersell V (2005) FOREGS geochemical atlas of Europe, part 1: background information, methodology and maps. Geological Survey of Finland. ISBN: 951-690-921-3

Salomons W, Förstner U (1984) Metals in the hydrocycle. Springer Verlag, Berlin, p 349. https://doi.org/10.1007/978-3-642-69325-0

Sánchez-Cabeza JA, Ruiz-Fernández AC (2012) 210Pb sediment radiochronology: an integrated formulation and classification of dating models. Geochim Cosmochim 82:183–200. https://doi.org/10.1016/j.gca.2010.12.024

Sanchez-Cabeza JA, Ruiz-Fernández AC, Ontiveros-Cuadras JF, Pérez Bernal LH, Olid C (2014) Monte Carlo uncertainty calculation of ^{210}Pb chronologies and accumulation rates of sediments and peat bogs. Quat Geochronol 23:80–93. https://doi.org/10.1016/j.quageo.2014.06.002

Santos IS, Garcia CAB, Passos EA, Alves JPH (2013) Distribution of trace metals in sediment cores from a hypertrophic reservoir in northeast Brazil. J Braz Chem Soc 24(2):246–255

Schroeder WH, Munthe J (1998) Atmospheric mercury - an overview. Atmos Environ 32:809–822. https://doi.org/10.1016/S1352-2310(97)00293-8

SE (1953) Séptimo censo general de población: 6 de Junio de 1950. Estado de Sonora. Secretaría de Economía, Dirección General de Estadística. pp 34 (in Spanish)

SE (2019) Sonora en la Minería. Secretaría de Economía, Gobierno del Estado de Sonora. http://economiasonora.gob.mx/portal/minero (Accessed in Oct 2020)

SEDESOL (2013) Municipios: Nacional. Unidad de Microrregiones. Cédulas de Información Municipal (SCIM). Secretaría de Desarrollo Social (in Spanish). http://www.microrregiones.gob.mx/zap/medioFisico.aspx?entra = nacion&ent = 26&mun = 018 (Accessed in June 2020)

SEMARNAT-INECC (2017) Generar información cualitativa y cuantitativa de las fuentes minero-metalúrgicas en México. Informe final. Instituto Nacional de Ecología y Cambio Climático, 217 pp (in Spanish). https://www.gob.mx/cms/uploads/attachment/file/329304/INFORME_FINAL_MERCURIO.pdf

SGM (2002) Carta geológica-minera, Ciudad Obregón G12-3, Sonora, Chihuahua y Sinaloa. Servicio Geológico Mexicano (in Spanish)

SGM (2015) Cartas Geoquímicas del Estado de Sonora (in Spanish). https://www.sgm.gob.mx/CartasDisponibles/ (Accessed in Jun 2020).

SGM (2018) Panorama Minero del Estado de Sonora. Subsecretaria de minería. pp 72 (in Spanish)

SINA (2020) Sistema Nacional de Información del Agua. Monitoreo de las Principales Presas de México. Presa Álvaro Obregón, Son. (El Oviachic) (in Spanish). http://sina.conagua.gob.mx/sina/almacenamientoPresas.php (Accessed in Jun 2020)

Soto-Jiménez MF, Hibdon S, Rankin CW, Aggarawl J, Ruiz-Fernández AC, Páez-Osuna F, Flegal R (2006) Chronicling a century of lead

pollution in Mexico: stable lead isotopic composition analyses of dated sediment cores. Environ Sci Technol 40:764–770

Szarlowicz K, Reczynski W, Czajka A, Spyt B, Szacilowski G (2018) Comprehensive study of the mountainous lake sediments in relation to natural and anthropogenic processes and time (Maly Staw Lake, Poland). Environ Sci Pollut R 25:3335–3347. https://doi.org/10.1007/s11356-017-0711-x

UNSCEAR (2000) Report to the General Assembly, with Scientific Annexes. United Nations Scientific Committee on the Effects of Atomic Radiation. United Nations, NewYork. pp 659

USEPA (1997) EPA's national hardrock mining framework. U.S. Environment Protection Agency. pp 177

Valdez-Zamudio D, Guertin DP (2000) Soil erosion studies in Buffelgrass pastures. USDA Forest Service Proceedings RMRS-P-13. 2000, 282-286. https://www.fs.fed.us/rm/pubs/rmrs_p013/rmrs_p013_282_286.pdf

van Afferden M, Hansen AM, Fuller CC (2005) Reconstrucción de la deposición atmosférica histórica de DDT en la Laguna de Zempoala en el centro de México. Ingeniería Hidrául 20(3):71–83

Wang C, Liu S, Zhao Q, Deng L, Dong S (2012) Spatial variation and contamination assessment of heavy metals in sediment in the Manwan Reservoir, Lancang River. Ecotox Environ Safe 82:32–39. https://doi.org/10.1016/j.ecoenv.2012.05.006

Yang H, Rose NL, Battarbee RW (2002) Distribution of some trace metals in Lochnagar, a Scottish mountain lake ecosystem and its catchment. Sci Total Environ 285:197–208. https://doi.org/10.1016/S0048-9697(01)00931-7

Publisher's note Springer Nature remains neutral with regard to jurisdictional claims in published maps and institutional affiliations.